# Supporting information

## A QM/MM Study of the Catalytic Mechanism of α-1,4-Glucan Lyase from *Gracilariopsis lemaneiformis*

Hao Su[a], Lihua Dong[a], Yongjun Liu*[a, b]

[a]*School of Chemistry and Chemical Engineering, Shandong University, Jinan, Shandong 250100, China*
[b]*Key Laboratory of Tibetan Medicine Research, Northwest Institute of Plateau Biology, Chinese Academy of Sciences, Xining, Qinghai 810001, China*

Table S1 Main distances and dihedral angles around the anomeric carbon (C1), and charges of atoms C1, C2, O5 at each stationary point along the reaction pathway for Model 1.

| | R | TS1 | IM1 | TS2 | IM2 | TS3 | IM3 | TS4 | IM4 | TS5 | P |
|---|---|---|---|---|---|---|---|---|---|---|---|
| | | | | | Distance(Å) | | | | | | |
| **C1-O5** | 1.38 | 1.30 | 1.25 | 1.26 | 1.35 | 1.27 | 1.25 | 1.24 | 1.24 | 1.28 | 1.35 |
| **C1-C2** | 1.53 | 1.52 | 1.51 | 1.52 | 1.54 | 1.52 | 1.51 | 1.50 | 1.50 | 1.39 | 1.32 |
| | | | | | Dihedral angle(º) | | | | | | |
| **H1-C1-O5-C2[a]** | -117.4 | -136.9 | 174.1 | 167.1 | 128.1 | 156.5 | 172.8 | -172.6 | -173.9 | -170.5 | -176.9 |
| **O2-C2-C3-C1[b]** | -128.2 | -131.3 | -128.1 | -127.8 | -130.1 | -126.9 | -127.6 | -129.9 | -129.0 | -145.6 | 171.6 |
| | | | | | Charge(e) | | | | | | |
| **C1** | 0.54 | 0.67 | 0.77 | 0.75 | 0.55 | 0.71 | 0.76 | 0.77 | 0.77 | 0.60 | 0.17 |
| **C2** | 0.08 | 0.04 | 0.05 | 0.07 | 0.15 | 0.08 | 0.05 | -0.00 | -0.01 | -0.09 | 0.20 |
| **O5** | -0.67 | -0.63 | -0.57 | -0.59 | -0.66 | -0.61 | -0.58 | -0.60 | -0.55 | -0.60 | -0.64 |

[a]θ1: H1-C1-O5-C2; [b]θ2: O2-C2-C3-C1.

Table S2 Main distances and dihedral angles around the anomeric carbon (C1), and charges of atoms C1, C2, O5 at each stationary point along the reaction pathway for Model 2.

| | **IM2-1** | **TS3-1** | **IM3-1** | **TS4-1** | **IM4-1** | **TS5-1** | **P-1** |
|---|---|---|---|---|---|---|---|
| | | | Distance(Å) | | | | |
| **C1-O5** | 1.34 | 1.29 | 1.24 | 1.23 | 1.23 | 1.27 | 1.35 |
| **C1-C2** | 1.54 | 1.52 | 1.51 | 1.50 | 1.50 | 1.39 | 1.31 |
| | | | Dihedral angle(º) | | | | |
| **H1-C1-O5-C2**[a] | 127.3 | 141.1 | 170.7 | 179.4 | 179.1 | -173.1 | -179.9 |
| **O2-C2-C3-C1**[b] | -128.5 | -125.2 | -124.9 | -126.2 | -125.2 | -141.7 | 178.9 |
| | | | Charge(e) | | | | |
| **C1** | 0.55 | 0.64 | 0.74 | 0.74 | 0.74 | 0.56 | 0.19 |
| **C2** | 0.14 | 0.08 | 0.05 | 0.00 | 0.00 | -0.08 | 0.22 |
| **O5** | -0.66 | -0.63 | -0.55 | -0.53 | -0.53 | -0.58 | -0.64 |

[a]θ1: H1-C1-O5-C2; [b]θ2: O2-C2-C3-C1.

Table S3 The energies of dispersion correction calculated by DFT-D3 program.

| Structure | Energy of dispersion correction (kcal/mol) | Relative value of Energy dispersion to R, R′ or IM2-1 (kcal/mol) |
|---|---|---|
| R | -111.7135 | 0.0 |
| TS1 | -112.6676 | -0.95 |
| IM1 | -111.9258 | -0.21 |
| TS2 | -112.0589 | -0.35 |
| IM2 | -111.3630 | 0.35 |
| TS3 | -112.5453 | -0.83 |
| IM3 | -111.8399 | -0.13 |
| TS4 | -111.4616 | 0.25 |
| IM4 | -111.3217 | 0.39 |
| TS5 | -111.4953 | 0.22 |
| P | -108.6871 | 3.03 |
| | | |
| R′ | -156.4925 | 0.00 |
| TS1′ | -157.0464 | -0.55 |
| IM1′ | -156.1530 | 0.34 |
| TS2′ | -156.2588 | 0.23 |
| IM2′ | -155.8934 | 0.60 |
| TS3′ | -156.7416 | -0.25 |
| IM3′ | -156.0657 | 0.43 |
| TS4′ | -157.4679 | -0.98 |
| IM4′ | -158.6307 | -2.14 |
| TS5′ | -157.7386 | -1.25 |
| P′ | -155.0130 | 1.48 |
| | | |
| IM2-1 | -72.5882 | 0.00 |
| TS3-1 | -72.6893 | -0.10 |
| IM3-1 | -72.2951 | 0.29 |
| TS4-1 | -71.1923 | 1.40 |
| IM4-1 | -71.7338 | 0.85 |
| TS5-1 | -72.6658 | -0.08 |
| P-1 | -71.4242 | 1.16 |

Fig. S1 Time dependence of RMSD from 10ns MD simulations of enzyme-substrate Michaelis complex.

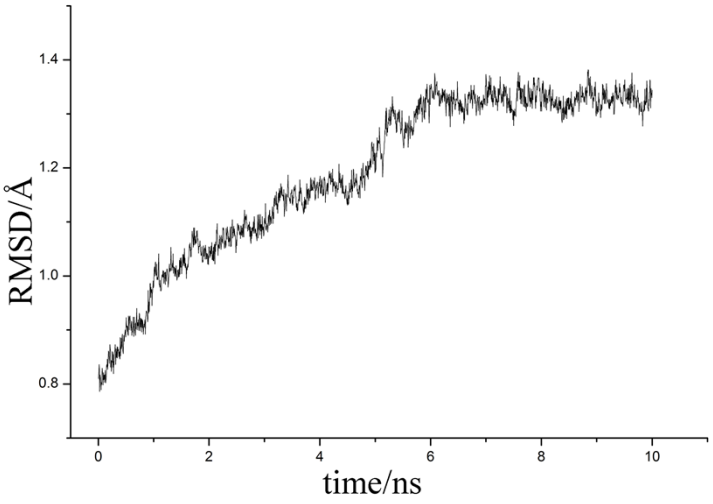


Fig. S2 The superposition of the active sites of 11 optimized geometries. These structures were taken firstly from the snapshots of MD simulation at interval of 200ps from 8ns to 10ns, and then optimized by QM/MM method at the level of B3LYP/ 6-31G(d,p) for QM region and CHARMM22/CMAP force field for MM region. An average structure was firstly derived from the 11 optimized geometries, and then the RMSDs of the 11 structures relative to the average one was calculated, which are 0.44, 0.404, 0.411, 0.378, 0.402, 0.392, 0.407, 0.397, 0.377, 0.390 and 0.397Å for 8.0, 8.2, 8.4, 8.6, 8.8, 9.0, 9.2, 9.4, 9.6, 9.8 and 10 ns, respectively. Since the RMSD at 9.6ns corresponds to the smallest value (0.377 Å), therefore, the structure at 9.6ns was thought to be representative and was used for the study of reaction pathway, which is shown in green.

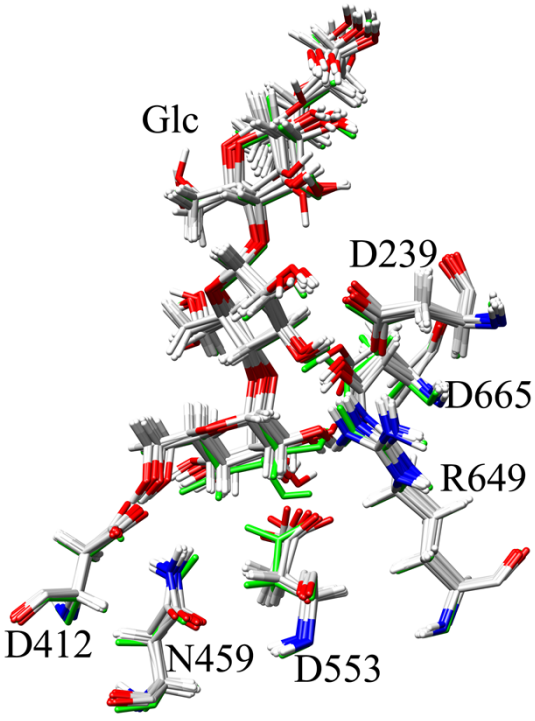

Fig.S3 B3LYP /6-31G(d,p)//CHARMM22 energy profile for the reaction that D553 acts as nucleophilic to trigger the reaction. In the scanning of profile, the reaction coordinate was defined by the difference of r1(O1···C1) and r2(C1···OB). For clarity, only part of the residues was presented in the structures. The bond lengths are shown in angstrom.

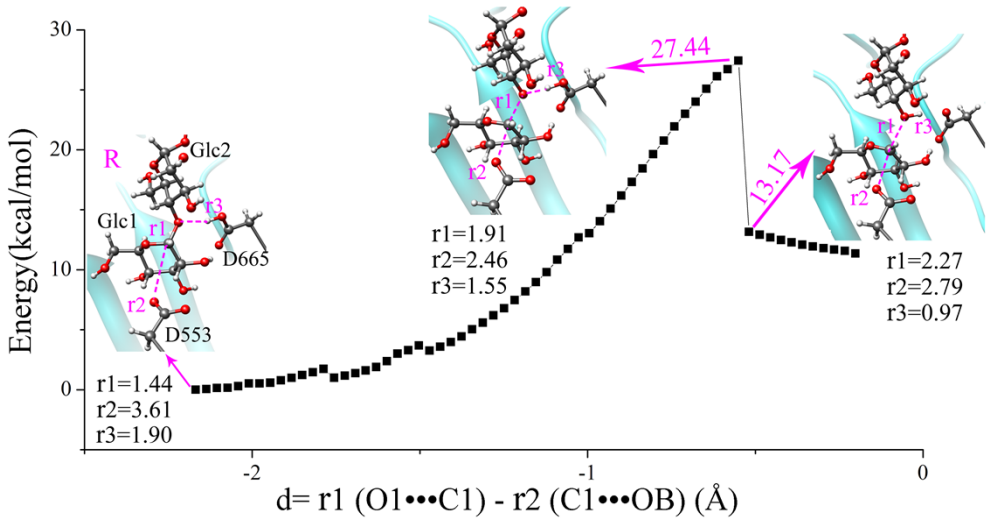


Fig. S4 Time dependence of RMSD from 8ns MD simulations of structure of IM2, in which the maltotriose group was removed from the active site.

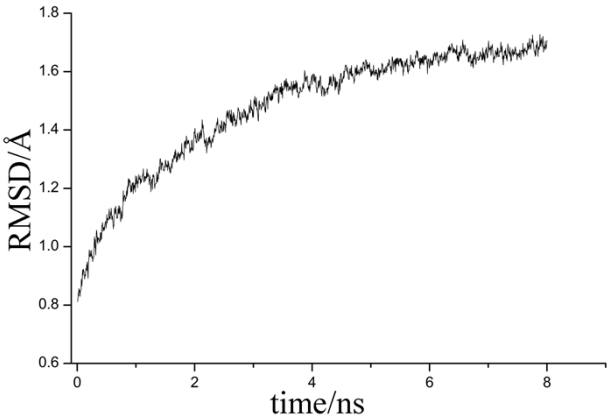

Fig.S5 The selected QM region for large QM region calculation.

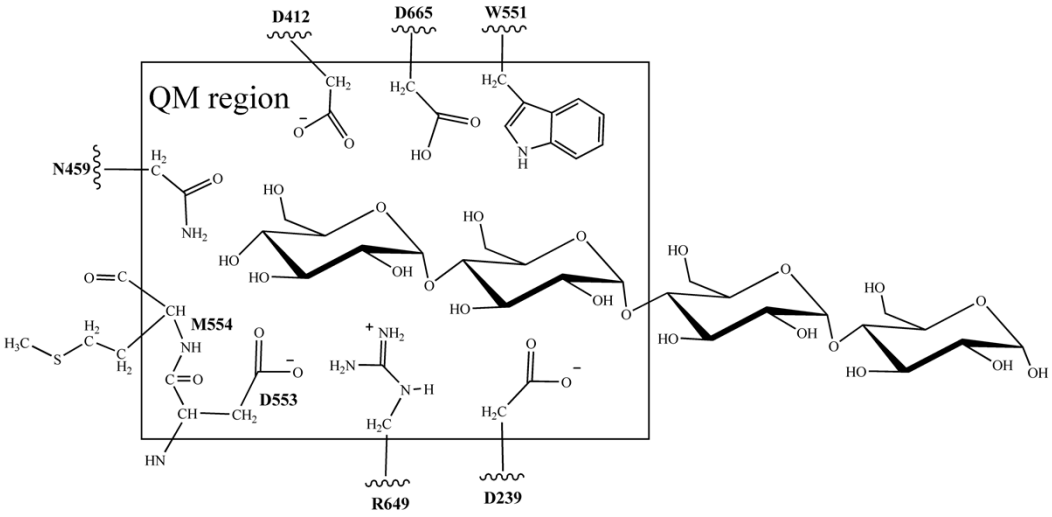


Fig.S6 The QM/MM optimized active site structure of Glase (denoted as R′ ), in which a large QM region (Model 3) was used. The key distances are shown in angstrom. Hydrogen bonds were shown in black dash lines.

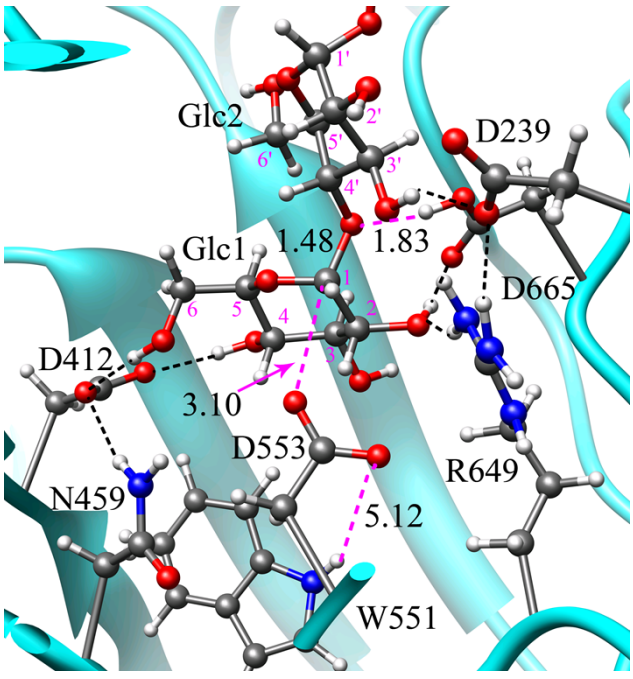


R′

Fig. S7 Optimized structures of transition states (TS1', TS2') and intermediates (IM1', IM2') for glycosylation step by using Model 3.

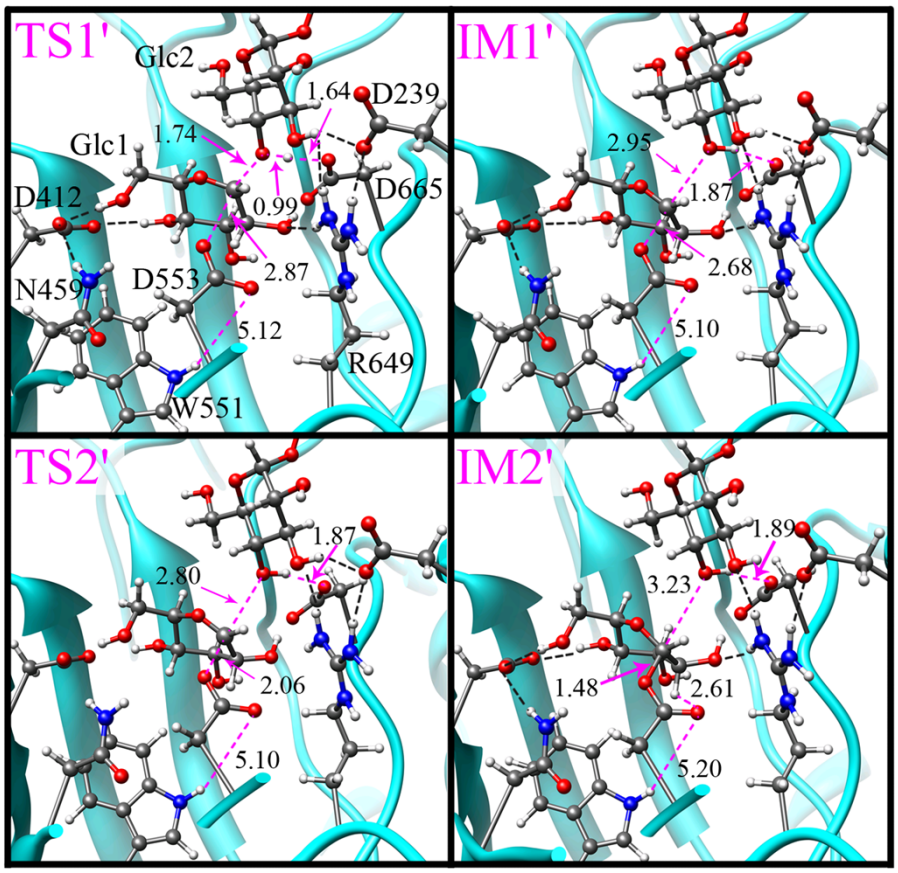

Fig. S8 The optimized structures of transition states, intermediates and product for deglycosylation step by using Model 3. Distances are given in angstrom.

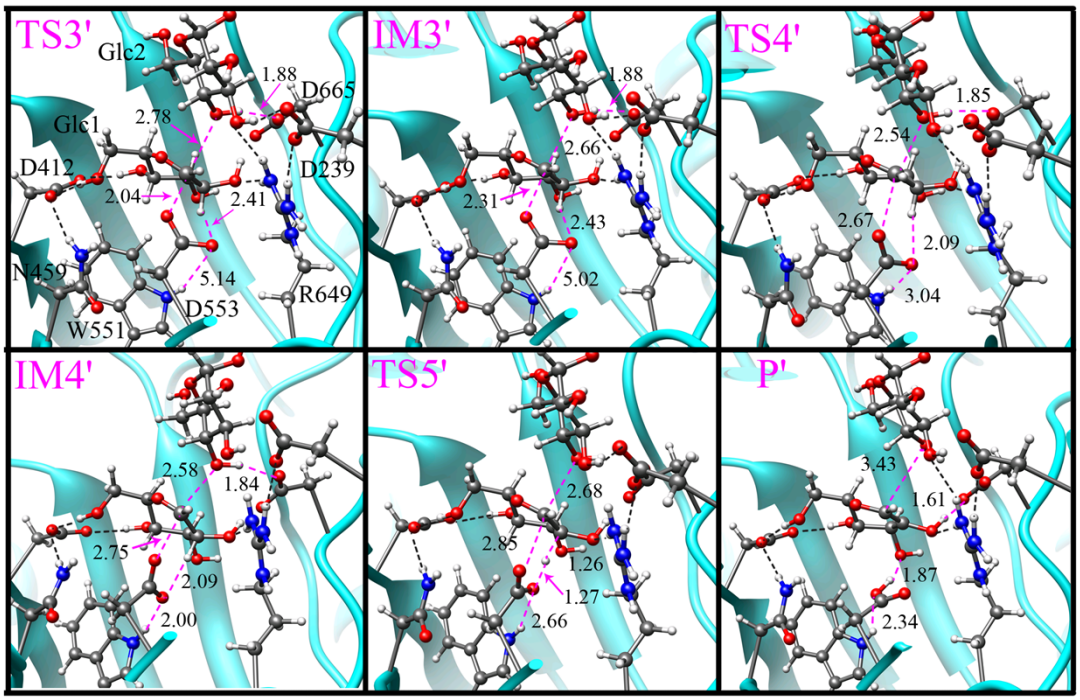


Fig.S9 The energy profiles of the reaction by using Model 3.